Annals of Biomedical Engineering (© 2010)
DOI: 10.1007/s10439-010-0158-4

Biotransport Phenomena in Freezing Mammalian Oocytes

GEER YANG,[1,2,4] MONIKA VERES,[3] GABOR SZALAI,[3] AILI ZHANG,[4] LISA X. XU,[4] and XIAOMING HE[1,2]

[1]Department of Mechanical Engineering, University of South Carolina, 300 Main Street, Columbia, SC 29208, USA; [2]Biomedical Engineering Program, University of South Carolina, Columbia, SC 29208, USA; [3]Department of Biological Sciences, University of South Carolina, Columbia, SC 29208, USA; and [4]Department of Biomedical Engineering, Shanghai Jiao Tong University, Shanghai 200240, China

(*Received 12 July 2010; accepted 31 August 2010*)

Associate Editor Tingrui Pan oversaw the review of this article.

Abstract—Water transport across the cell plasma membrane and intracellular ice formation (IIF)—the two biophysical events that may cause cell injury during cryopreservation—were studied by cryomicroscopy and modeling using mammalian (*Peromyscus*) oocytes. Unusually high activation energy for water transport across the cell plasma membrane was identified indicating that the water transport process is unusually sensitive to temperature (and cooling rate). Although literally all studies on IIF were conducted using protocols with ice-seeding (seeding extracellular ice usually at ≥−7 °C), it is not used for cell cryopreservation by vitrification that is becoming increasingly popular today. In this article, we show that ice-seeding has a significant impact on IIF. With ice-seeding and cooling at 60 °C/min, IIF was observed to occur over a wide range from approximately −8 to −48 °C with a clear change of the ice nucleation mechanism (from surface- to volume-catalyzed nucleation) at approximately −43 °C. On the contrary, without ice-seeding, IIF occurred over a much narrower range from approximately −19 to −27 °C without a noticeable change of the nucleation mechanism. Moreover, the kinetics of IIF without ice-seeding was found to be strongly temperature (and cooling rate) dependent. These findings indicate the importance of quantifying the IIF kinetics in the absence of ice-seeding during cooling for development of optimal vitrification protocols of cell cryopreservation.

Keywords—Water transport, Intracellular ice formation (IIF), Cryomicroscopy, Modeling, Cryopreservation, Vitrification.

INTRODUCTION

Oocyte cryopreservation is of great importance to the advancement of assisted reproductive medicine and maintenance of animal resources and endangered species.[33,42,48,61] However, the outcome of oocyte cryopreservation has been largely dismal so far.[13,17,18,37,39,52] The two major biophysical events that may result in damage to oocytes during cryopreservation is the formation of a significant amount of ice inside the cells (intracellular ice formation or IIF) and excessive cell dehydration as a result of water transport out of the cells.[47,56] Conventionally, oocyte cryopreservation was done by the so-called slow-freezing approach which relies on the use of an optimal slow cooling rate (usually <2 °C/min) to dehydrate the cells so that IIF can be minimized while, at the same time, without incurring significant cell damage by excessive cell dehydration. As the slow-freezing approach is unable to completely avoid cell injury due to either IIF or excessive cell dehydration,[47] cryopreservation by vitrification is becoming increasingly popular as an alternative to slow freezing for long-term preservation of oocytes.[9,43,50,62]

Vitrification is the non-equilibrium transition of liquid water into a metastable, amorphous glass rather than ice crystals. Conventionally, this was done by using an abnormally high concentration (4–7 M) of cryoprotectant (CPA).[14,53] However, such a high CPA concentration can cause significant osmotic and metabolic damages to oocytes within a few minutes.[6,7,15,16,27,29] As a result, efforts have been made to minimize the high CPA concentration induced cell injury using multiple CPAs and multiple steps of CPA loading with short CPA exposure time (restricted to a few minutes) in each step, which make the cryopreservation procedure complicated and difficult to control because it also takes a few minutes for the diffusion of CPA into oocytes to reach equilibrium.[24,27,32,51] More recently, research has been done to achieve cell vitrification at a much-reduced (and much less toxic) CPA concentration (≤1.5–2.5 M) (low-CPA vitrification) with promising outcomes. This can be done by cooling the cells at an ultrafast cooling rate (≥10^5 °C/min)

Address correspondence to Xiaoming He, Department of Mechanical Engineering, University of South Carolina, 300 Main Street, Columbia, SC 29208, USA. Electronic mail: xmhe@sc.edu

Published online: 17 September 2010

and/or confining the cells in sub-nanoliter space.[24,67] The low-CPA vitrification approach should combine all the advantages of slow-freezing and conventional vitrification using a high concentration of CPAs while avoiding all their shortcomings.

Although studies have been reported on quantifying water transport across the plasma membrane of a variety of cells during freezing,[4,19,21] it has not been done for the *Peromyscus* oocytes. Compared to water transport, quantitative studies on IIF have been scarce in the literature.[56] Moreover, literally all the studies on IIF were performed using freezing protocols with an ice-seeding step (i.e., seeding extracellular ice at a high subzero temperature usually ≥–7 °C).[56] Although such an ice-seeding step is required to achieve the optimal outcome for slow-freezing, it should be excluded from the protocol for cryopreservation by vitrification. This is because the goal of vitrification is to eliminate both intra- and extracellular ice formation altogether. Therefore, it is of great importance and interest to understand how ice-seeding will affect the kinetics of IIF.

In this study, the two biophysical processes (i.e., water transport across the cell plasma membrane and IIF) during freezing *Peromyscus* oocytes were investigated using cryomicroscopy and by modeling. Our results show that ice-seeding at a high subzero temperature has a significant impact on IIF, suggesting that the existing data on IIF reported in the literature obtained using freezing protocols with ice-seeding might not be applicable for studying IIF during vitrification.

MATERIALS AND METHODS

Animals

The outbred virgin *Peromyscus* (deer mouse) *maniculatus bairdii* animals were obtained from the collection of the *Peromyscus* Genetic Stock Center at the University of South Carolina (Columbia, SC), where they were maintained at 16–8 h light–dark cycle.

Chemicals

Pregnant mare serum gonadotropin (PMSG) and human chorionic gonadotropin (hCG) were obtained from the National Hormone & Peptide Program (Harbor-UCLA Medical Center, LA, CA). The M2 culture medium for oocytes was purchased from Sigma–Aldrich (St. Louis, MO).

Isolation of Peromyscus Oocytes

The procedure for isolation of the *Peromyscus* oocytes was reported elsewhere.[63] In brief, 12–24-week-old virgin *Peromyscus maniculatus bairdii* females were hormone primed with 15 IU of PMSG followed by a second 15 IU of PMSG 24 h later. At 48 h post the second PMSG, the females were further hormone primed with 15 IU of hCG. At 24 h after the hCG injection, the females were cervically dislocated, and oviducts with an attached fragment of the uterus were excised. A 32-gauge blunted needle connected to a 1-cc or 3-cc glass syringe was inserted into the infundibulum, and the oocytes were flushed with M2 medium pre-warmed to 37 °C. Approximately six mature oocytes were isolated per animal on average. All the procedures for the isolation of oocytes were approved by the Institutional Animal Care and Use Committee (IACUC) at the University of South Carolina.

Cryomicroscopy Study of Cell Dehydration and Intracellular Ice Formation (IIF)

For cryomicroscopy studies, a small drop (~5 μL) of culture medium with *Peromyscus* oocytes was pipetted into the center of a quartz crucible (15 mm in diameter). Within a few seconds, the oocytes sunk down on the bottom surface of the crucible because they are heavier than the carrying solution. The crucible (bottom) was then placed on the top surface of a Linkam (Waterfield, UK) BCS 196 cryostage mounted on an Olympus BX 51 microscope for real-time monitoring during freezing.

The cryomicroscopy studies were performed to investigate both dehydration (or water transport across the plasma membrane) of *Peromyscus* oocytes during freezing with ice-seeding under three different cooling rates (0.5, 6, and 60 °C/min) and IIF during freezing the cells at a cooling rate of 60 °C/min either with or without ice-seeding.

To study freezing-induced cell dehydration (or water transport) and IIF with ice-seeding, the oocytes were first cooled to −4 °C at 10 °C/min followed by holding at −4 °C to seed ice using a syringe needle pre-cooled in liquid nitrogen. After 2 min post ice-seeding, the cells were warmed up to −2 °C at 10 °C/min to minimize the initial cell dehydration as a result of ice-seeding and for better visualization of the cells during further freezing. After equilibrating at −2 °C for 2 min, the cells were cooled to a deep subzero temperature (down to −60 °C) at 0.5, 5, or 60 °C/min. Finally, the cells were thawed by heating to room temperature at 10 °C/min. For the study on IIF without ice-seeding, cells were cooled to 0 °C at 10 °C/min, held for 5 min to achieve equilibrium, further cooled to −50 °C at 60 °C/min, and finally heated back to room temperature at 10 °C/min. The whole cooling and heating processes were observed with a 10× long working distance objective and recorded

using a Qimaging (Survey, BC, Canada) QICAM CCD microscope camera at full resolution every one and 20 s for the IIF and water transport studies, respectively.

Modeling of Water Transport During Freezing

Water transport across the cell plasma membrane (leading to cell dehydration) during freezing was modeled using the following equations[34,40,45]:

$$\frac{dV_c}{dT} = -\frac{L_p A_c RT}{Bv_w} \times \left[\frac{\Delta H_f}{R}\left(\frac{1}{T_R}-\frac{1}{T}\right) - \ln\frac{V_c - V_b - V_s}{V_c - V_b - V_s + \phi_s n_s v_w}\right] \quad (1)$$

$$L_p = L_{pg}\exp\left[-\frac{E_{Lp}}{R}\left(\frac{1}{T}-\frac{1}{T_R}\right)\right] \quad (2)$$

where T is the temperature (in K), V is the volume, A is the cell surface area, B is the cooling rate, n is the molar amount, v is the molar volume (18 mL/mol for water), ΔH_f is the molar enthalpy of fusion of water (6016.52 J/mol), R is the universal gas constant (8.314 J mol^{-1} K^{-1}), and T_R is a reference temperature (272.59 K), ϕ is the dissociation constant of salt (2 for NaCl), L_{pg} is the water permeability of cell plasma membrane at T_R, E_{Lp} is the activation energy for water transport across cell plasma membrane, V_b is the osmotically inactive volume in cells, and the subscripts c, s, and w represent the cell, the solute, and the water, respectively. Among the various parameters, L_{pg}, E_{Lp}, and V_b are the three model parameters that are cell type-dependent and they need to be determined using experimental data.

Modeling the Probability of IIF During Freezing

As with any crystallization process, ice formation in cells involves two consecutive steps: nucleation to form ice nuclei, and the subsequent growth of the nuclei. When freezing cells in isotonic solutions at a cooling rate less than a few hundred Celsius per minute, ice nucleation is the rate-limiting step of IIF. In other words, once ice nuclei form in cells, they will grow instantly to result in significant IIF that is manifested as darkening of the cell cytoplasm under a bright field of light microscopy. Nucleation of ice in cells can be either surface-catalyzed nucleation (SCN) or volume-catalyzed nucleation (VCN), and the probability (P_{IIF}) of IIF can be modeled as follows[56,57]:

$$P_{IIF} = P_{IIF}^{SCN} + \left(1 - P_{IIF}^{SCN}\right)P_{IIF}^{VCN} \quad (3)$$

$$P_{IIF}^{SCN} = 1 - \exp\left[-\int_0^t A_c I^{SCN} dt\right] = 1 - \exp\left[-\int_T^{T_{f0}} A_c I^{SCN}(1/B)dT\right] \quad (4)$$

$$P_{IIF}^{VCN} = 1 - \exp\left[-\int_0^t V_c I^{VCN} dt\right] = 1 - \exp\left[-\int_T^{T_{f0}} V_c I^{VCN}(1/B)dT\right] \quad (5)$$

where t is the time, T_{f_0} is the equilibrium freezing temperature of isotonic solutions (272.59 K), and I is the ice nucleation rate that can be modeled using the following equation for both SCN and VCN[56,57]:

$$I^{XCN} = \Omega_0^{XCN}\frac{N^{XCN}}{N_0^{XCN}}\frac{\eta_0}{\eta}\left(\frac{T}{T_{f_0}}\right)^{0.5}\exp\left[\frac{-\kappa_0^{XCN}(T_f/T_{f_0})^4}{(T-T_f)^2T^3}\right] \quad (6)$$

where T_f is the equilibrium freezing temperature of the cytoplasm during freezing, N and N_0 are the number of water molecules either in the cells (for VCN) or in contact with the cell plasma membrane (for SCN) during and before freezing, respectively (the ratio of N to N_0 is equal to 1 if cell dehydration during freezing is negligible), the superscript XCN represents either SCN or VCN, Ω_0 and κ_0 are, respectively, the kinetic and thermodynamic model parameters that need to be determined using experimental data, η_0 is viscosity of the cell cytoplasm at T_{f_0} under isotonic condition, and η is viscosity of the cell cytoplasm during freezing and can be estimated using the following equation[34]:

$$\eta = \eta_w\exp\left(\frac{2.5\varphi_s}{1-0.61\varphi_s}\right) \quad (7)$$

where φ_s is the volume fraction of salts, and η_w is the viscosity of water that can be calculated using the free volume model as follows[26]:

$$\eta_w = \eta_{w,0}\exp\left(\frac{v_w^*}{(K_{11}/\lambda)(K_{21}-T_{gw}+T)}\right) \quad (8)$$

where $\eta_{w,0}$ is a pre-exponential constant (3.33×10^{-5} Pa s), v_w^* is the specific volume of water at 0 K (0.91 mL/g), K_{11}/λ (1.945 mL g^{-1} K^{-1}) and K_{21} (−19.73 K) are the two free volume parameters for water, and T_{gw} is the glass transition temperature of water (136 K).

Determination of Model Parameters

The model parameters for water transport (L_{pg}, E_{Lp}, and V_b) and IIF (Ω_0^{SCN}, κ_0^{SCN}, Ω_0^{VCN}, and κ_0^{VCN}) were determined by fitting the above models, respectively, to experimental data on the cell volume and the probability of IIF as a function of temperature during freezing obtained from the cryomicroscopy studies. The fitting was done with a non-linear optimization procedure (the flexible tolerance method[28]) to minimize the root mean square between the model predictions and the experimental data, which has been used by the authors in a number of studies to extract multiple parameters in a variety of models for various applications.[22,23,25,26]

RESULTS AND DISCUSSION

Cryomicroscopy Study of Water Transport/Cell Dehydration

Figure 1 shows typical micrographs of a *Peromyscus* oocyte in culture medium (a) before cooling, (b) at −2 °C after seeding extracellular ice, (c) at −9 °C during freezing, and (d) at 22 °C after thawing. Clearly, after seeding ice and during freezing, the cells become shrunken due to the formation of extracellular ice that freeze-concentrates the extracellular solution and are deformed presumably due to the formation of large (tens of microns) extracellular ice crystals (asterisks in Figs. 1b and 1c).

To quantify the cell (cytoplasm) volume, the irregular area of the deformed cytoplasm (indicated by arrows in Figs. 1b and 1c) was measured using the Linksys software specially designed for the cryomicroscopy system by Linkam (Waterfield, UK) and an equivalent diameter was calculated by assuming the area to be circular. The volume of the deformed cytoplasm was then estimated by assuming a spherical geometry. Although these assumptions inevitably introduce some error, it is the best available approach for studying freezing-induced dehydration in oocytes. Another method that has been commonly used to study water transport during freezing is DSC (differential scanning calorimetry).[10,11] However, the DSC-based method usually requires the presence of thousands of cells in a sample. As a result, it is difficult to apply for studying the water transport process during freezing mammalian oocytes since the number of oocytes available is usually small (<~100 per isolation for *Peromyscus*).

The normalized cell volume (i.e., the ratio of the cell volume during freezing to the initial cell volume) as a function of temperature at three different cooling rates is shown in Fig. 2 as symbols. It is interesting and important to note that there is a significant drop

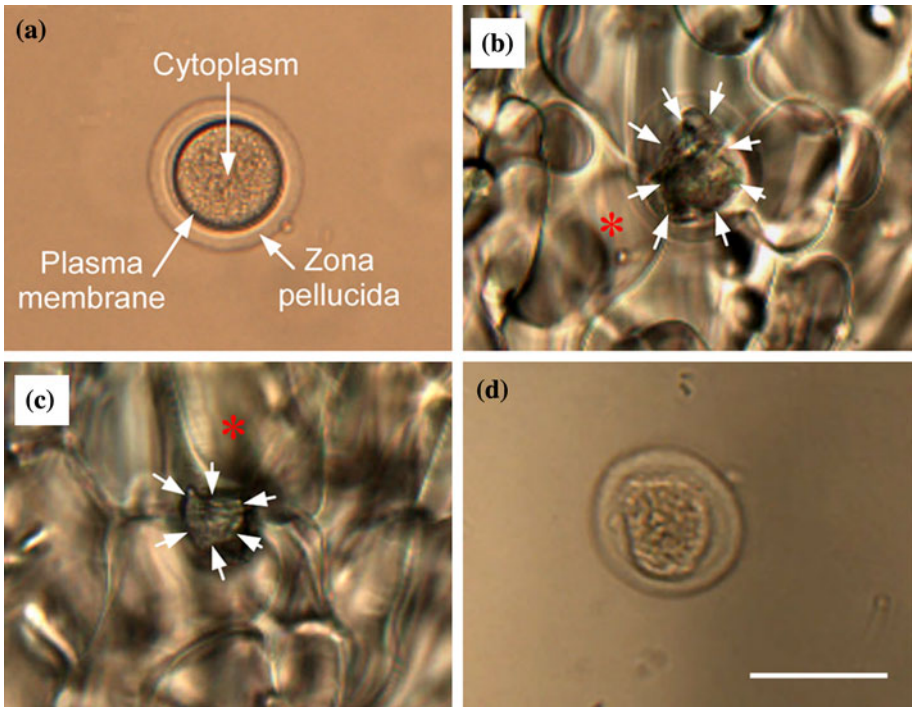

FIGURE 1. Typical micrographs showing a *Peromyscus* oocyte in culture medium (a) at 22 °C before cooling, (b) at −2 °C after ice-seeding, (c) at −9 °C during freezing, and (d) at 22 °C after thawing: Cooling rate, 0.5 °C/min; arrows indicate the boundary of cell cytoplasm; asterisks indicate ice crystals, and scale bar, 100 μm.

(~30%) in the cell volume after ice-seeding and equilibrating at −2 °C although the subcooling is only ~1.5 °C (the equilibrium freezing temperature is −0.56 °C). With the further decrease of temperature, the cells dehydrated further and significantly when cooled at both 0.5 (Fig. 1c) and 5 °C/min particularly above −5 °C. However, further dehydration beyond that of ice-seeding is negligible (~2%) when the cells were cooled at 60 °C/min. The cell volume did not change much at all with further cooling beyond −15 °C for all the three cooling rates tested. Moreover, the final cell volume is strongly dependent on the cooling rate (i.e., both time and temperature during freezing) used.

After thawing, the cells lost their morphologic polarity (or heterogeneity, Fig. 1d) and appeared degenerated under all the cooling rates studied, which indicates the necessity of cryoprotectant to protect the cells during freezing. When the cells were cooled at 0.5 °C/min, no apparent IIF was observed indicating that the cells were damaged as a result of excessive cell dehydration. At 60 °C/min, no further significant cell dehydration beyond that after ice-seeding was observable, indicating that the cells were damaged by significant IIF (to be discussed further later). The cells cooled at 5 °C/min were damaged by both cell dehydration and IIF (data not shown). Similar phenomena have been observed when freezing metaphase II mouse oocytes in isotonic solutions.[60]

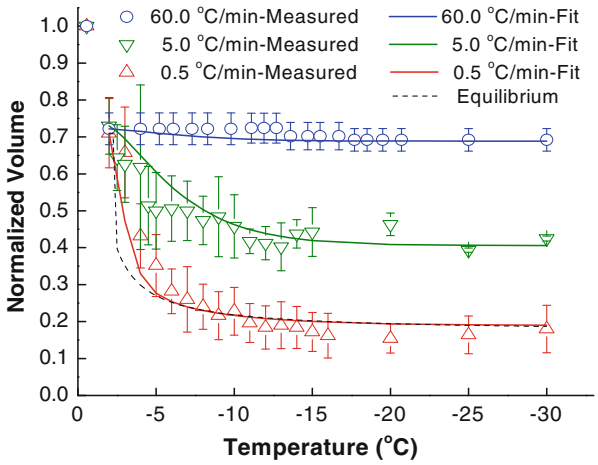

FIGURE 2. The ratio of oocyte volume during freezing to the initial cell volume before freezing in culture medium at three different cooling rates (0.5, 5 and 60 °C/min): The symbols represent the experimental data (mean ± SD, $n = 5$); solid lines are fitting results; and dashed line represents the equilibrium freezing conditions predicted using an extremely slow cooling rate (0.01 °C/min).

Modeling of Water Transport/Cell Dehydration

The experimental data shown in Fig. 2 from the cryomicroscopy studies were fit using the water transport model (Eqs. (1)–(2)), and the results are also shown in the figure as solid lines ($R^2 = 0.965$). The resultant three model parameters (L_{pg}, E_{Lp}, and V_b/V_{Cell}) are listed in Table 1. With the three model parameters, we further predicted the change of the normalized volume with temperature at an extremely slow cooling rate (0.01 °C/min to approximate the equilibrium freezing condition), and the results are shown in Fig. 2 as a dashed line. Clearly, further decrease of the cooling rate to <0.5 °C/min will not significantly affect the temperature dependence of the freezing-induced dehydration of *Peromyscus* oocytes. Moreover, cell dehydration mainly occurred above −5 °C at such an extremely slow cooling rate, which explains the observed significant cell dehydration (~30%) after equilibrating the cells at −2 °C.

The three model parameters reported in the literature for oocytes (in isotonic solutions without cryoprotectant) of several other mammalian species are also shown in Table 1 for comparison. It is clear from the table that all the three parameters vary from species to species. The value of V_b/V_{Cell} for the various

TABLE 1. A comparison of the three model parameters of water transport obtained in this study for *Peromyscus* oocytes and that reported in the literature for some other oocytes.

Oocyte type	Ref.	$L_{pg} \times 10^{-14}$ ($m^3\ N^{-1}\ s^{-1}$)	E_{Lp} (kJ/mol)	V_b/V_{Cell}
Peromyscus (mature)	This study*	5.24 at −0.56 °C	196.5	0.169
Human (mature)	Hunter et al.[30,31]	15 at 37 °C 4.1 at 0 °C	14.1	0.29
Rhesus monkey (metaphase II)	Younis et al.[66]*	3.8 at 0 °C	141.5	0.1
	Karlsson et al.[35]	9.17 at 23.5 °C	n/d	0.197
Bovine (*in vitro* matured)	Ruffing et al.[54]*	4.1 at 0 °C	32.8	0.247
ICR mouse	Litkouhi et al.[41]	10.5 at 20 °C	n/d	0.247–0.28
	Benson and Critser[2]	6.58 at 22 °C	47.65	0.22
$B_6D_2F_1$ mouse (metaphase II)	Toner et al.[58]*	0.733 at 0 °C	55.7	0.214
	Leibo[38]	7.24 at 20 °C	60.7	0.18

L_{pg} reference water permeability, E_{Lp} activation energy of water transport, and V_b/V_{Cell} ratio of osmotically inactive volume to initial cell volume. References marked with asterisk (*) were done with freezing (i.e., extracellular ice formation).

oocytes varies between 0.1 and 0.3 and the value (0.169) obtained in this study is within the usual range. The critical parameters that govern the cell dehydration in response to freezing are the reference water permeability (L_{pg}) of the cell plasma membrane and the activation energy for water transport across the plasma membrane (E_{Lp}). The L_{pg} determined here for *Peromyscus* oocytes (5.24×10^{-14} m^3 N^{-1} s^{-1} at -0.56 °C) is similar to that of oocytes from large animals including mature human oocytes, metaphase II monkey oocytes, and *in vitro*-matured bovine oocytes at 0 °C, although it is more than seven times higher than that for the metaphase II oocytes from the small hybrid-inbred $B_6D_2F_1$ mouse at 0 °C. A high value of L_{pg} indicates a high permeability of the cell plasma membrane to water at the given reference temperature.

Unlike L_{pg}, the activation energy (E_{Lp}) for water transport across the plasma membrane of *Peromyscus* oocytes during freezing is much higher than that reported for all the other oocytes determined either with or without freezing (*Note*: in a few studies,[36,55] the activation energy determined under the freezing condition was reported to be higher than that at superzero temperatures, although the trend does not appear to apply to the $B_6D_2F_1$ mouse oocytes, listed in Table 1). According to Eq. (2), a higher E_{Lp} means that the plasma membrane water permeability will drop more with the decrease of temperature. In other words, the plasma membrane water permeability of *Peromyscus* oocytes can be much lower than that of mature human oocytes, metaphase II monkey oocytes, and *in vitro*-matured bovine oocytes at a subzero temperature (e.g., −5 °C) even though their plasma membrane has similar water permeability at the same reference temperature (i.e., ~0 °C).

Using Eq. (2) and the water transport parameters for the *Peromyscus* oocytes given in Table 1, the water permeability of the plasma membrane of the cells at −15 °C is found to be less than 1% of that at the reference temperature (−0.56 °C) (5.24×10^{-14} vs. 4.10×10^{-16} m^3 N^{-1} s^{-1}). In other words, the plasma membrane of the oocytes is essentially shut off to water transport at −15 °C, which may explain why the cell volume did not change much at all with further cooling beyond −15 °C for all the cooling rates shown in Fig. 2. Therefore, it is crucial to maintain a slow enough cooling rate (e.g., 0.5 °C/min) to sufficiently dehydrate the cells before the temperature becomes low enough to significantly slow down the water transport if maximum cell dehydration is the eventual goal. Otherwise, significant residual water will be retained in the cells (e.g., at 5 and 60 °C/min shown in Fig. 2) which renders the cells vulnerable to IIF during slow-freezing.

Cryomicroscopy Study of IIF: The Effect of Ice-seeding

Typical micrographs showing three *Peromyscus* oocytes in culture medium (a) before ice-seeding, (b) at −2 °C after ice-seeding, (c) at −11.1 °C during freezing, (d) at −14.7 °C during freezing, (e) at −11.6 °C during thawing, and (f) at room temperature after thawing are given in Fig. 3. Similar to what we

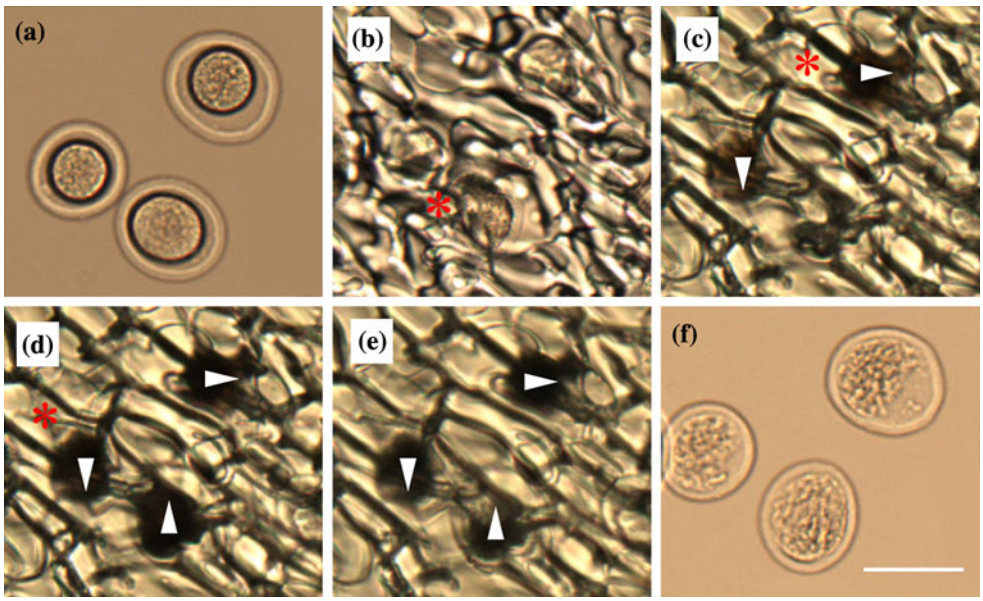

FIGURE 3. Typical micrographs showing three *Peromyscus* oocytes in culture medium (a) at 22 °C before cooling, (b) at −2 °C after ice-seeding, (c) at −11.1 °C during freezing, (d) at −14.7 °C during freezing, (e) at −11.6 °C during thawing, and (f) at 22 °C after thawing: Arrowheads indicate significant IIF (darkening); asterisks indicate extracellular ice crystals; and scale bar, 100 μm.

observed during the water transport study, the cells were deformed and shrunken at −2 °C after seeding extracellular ice (b), and no apparent intracellular ice was observable in any of the cells at the temperature. With further cooling, IIF occurred in two of the cells at −11.1 °C (arrowheads in c) and in all of the three cells at −14.7 °C (arrowheads in d). Moreover, the cells marked by the downward arrowhead appeared darker at −14.7 °C than at −11.1 °C, indicating IIF could continue to accumulate over a small temperature range in some of the cells. No apparent morphological change could be observed with further cooling to −60 °C and the subsequent heating until approximately −15 °C when the intracellular ice started melting with further heating (e.g., in the cell marked by the upward arrowhead in d and e). It is interesting to note that the intracellular ice formed in the cell marked by the upward arrowhead at a lower temperature also started thawing at a lower temperature than ice in the other two cells, presumably because the highest temperature required for maintaining phase equilibrium of the intracellular ice is dependent on the temperature at which the ice is initially formed. The three oocytes lost their structural polarity (or heterogeneity) and appeared degenerated (F) after thawing, which is not surprising as significant IIF is a lethal event to cells during freezing.

Typical micrographs showing the morphological change of three *Peromyscus* oocytes in culture medium (a) underwent freezing without ice-seeding are shown in Fig. 4. No significant IIF (or darkening) was observable at −18.6 °C when extracellular ice first formed (b). With a slight further cooling to −19.8 °C, significant IIF was observable in all the three cells (marked by arrowheads in c). In contrast to the significantly deformed morphology of the three *Peromyscus* oocytes during freezing with ice-seeding shown in Fig. 3, no apparent deformation was observable to the cells during freezing without ice-seeding. Presumably, this is due to the difference in the crystal size of extracellular ice between the two conditions: The crystals of extracellular ice were much bigger and more clearly visible in samples with ice-seeding (asterisks in Figs. 3b, 3c, and 3d) while they were much finer, and it is difficult to identify individual ice crystals in the samples with no ice-seeding during freezing (Figs. 4b and 4c). Moreover, significant IIF in the oocytes occurred usually at a temperature less than 3 °C lower than the temperature at which extracellular ice stochastically formed. Consequently, the time for water transport is short, and cell dehydration during freezing without ice-seeding is negligible. Of note, cell dehydration during freezing the *Peromyscus* oocytes without ice-seeding should be negligible regardless of the cooling rate used as long as the stochastic event of extracellular ice formation occurs below approximately −15 °C at which the cell plasma membrane is essentially shut off to water transport according to our cell dehydration studies (Fig. 2).

No apparent change in the intracellular ice was observable with further cooling of the cells to −50 °C (Fig. 4d) and the subsequent heating to ~−15 °C when an interesting phenomenon was consistently observed: The cell cytoplasm became much darker than that

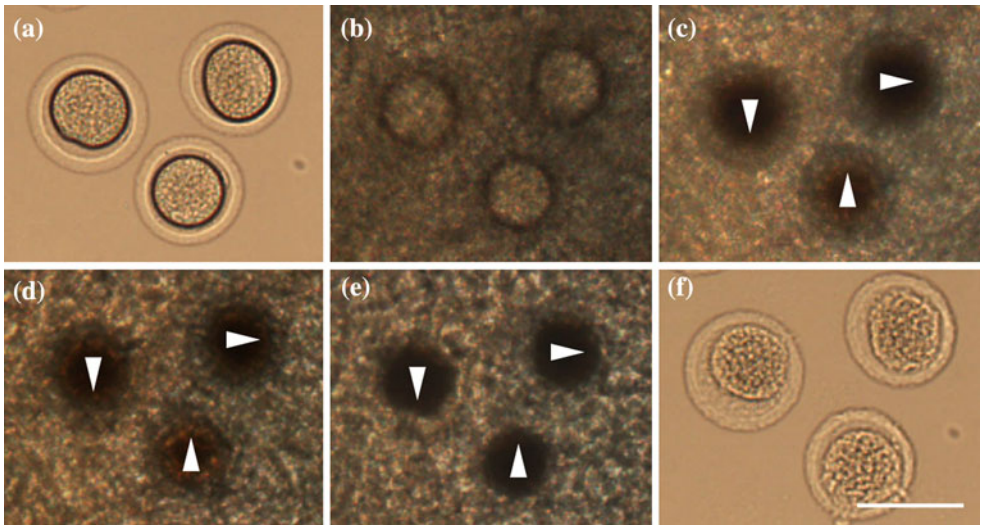

FIGURE 4. Typical micrographs showing three *Peromyscus* oocytes in culture medium (a) at 22 °C before cooling, (b) at −18.6 °C when extracellular ice first formed stochastically, (c) at −19.8 °C when significant IIF (darkening) occurred, (d) at −50 °C during freezing, (e) at −11 °C during thawing, and (f) at 22 °C after thawing: Arrowheads indicate significant IIF (darkening) and scale bar, 100 μm.

during freezing (Figs. 4e vs. 4d) with further heating to approximately −8 °C indicating more IIF during heating from −15 to −8 °C, which is in contrast to what we observed for the intracellular ice formed during freezing with ice-seeding. The latter started melting without apparent recrystallization when heated to above ~−15 °C (Fig. 3e). Presumably, the additional ice formation (recrystallization) in the cells during the warming phase is a result of the slow heating rate (10 °C/min) used in our experimental protocol. Further study is warranted to understand the effect of heating rate on the ice recrystallization process during the warming phase after freezing the cells without ice-seeding. The intracellular ice gradually disappeared with further heating from ~−8 °C to room temperature. As with the cells frozen with ice-seeding and thawed shown in Fig. 3f, the three oocytes appeared degenerated after thawing (Fig. 4f) presumably as a result of the significant IIF during both freezing and melting phases (Figs. 4c, 4d, and 4e).

The cumulative probability of IIF (P_{IIF}) as a function of temperature during freezing was further quantified, and the results are shown in Fig. 5 as symbols for both freezing with (triangle) and without (circle) ice-seeding. The data were obtained by pooling the temperature at which 50 and 59 oocytes became darkened (indicating significant IIF) for the freezing conditions with and without ice-seeding, respectively. Clearly, ice-seeding has a significant impact on the kinetics of IIF in the *Peromyscus* oocytes during freezing. Without ice-seeding, no IIF in the oocytes was observed until the cells were cooled to ~−19 °C and the event of IIF occurred over a small temperature range from ~−19 °C to −27 °C.

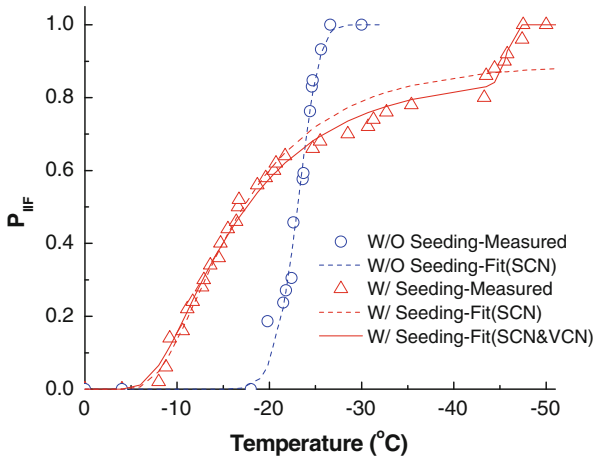

FIGURE 5. The cumulative probability of IIF (P_{IIF}) in *Peromyscus* oocytes: The symbols are experimental data for freezing either with (*triangle*) or without (*circle*) ice-seeding; the dashed lines are fitting results considering only the SCN; the solid line is the fitting result considering both SCN and VCN; and the experimental data were pooled from a total of 50 and 59 oocytes (isolated from at least 20 animals) for the conditions with and without ice-seeding, respectively.

On the contrary, with ice-seeding, significant IIF in the *Peromyscus* oocytes started at a much higher subzero temperature (~−8 °C) and occurred over a much wider temperature range from ~−8 to −48 °C. Moreover, there is an apparent kink point (at ~−43 °C) where the slope of P_{IIF} vs. temperature increased abruptly, indicating that there is a change of the dominant ice nucleation mechanism for IIF at ~−43 °C when freezing the *Peromyscus* oocytes at 60 °C/min with ice-seeding. Presumably, the SCN dominates above −43 °C, while below −43 °C, it is the VCN that dominates according to the classical two-mechanism theory of IIF during freezing.[59] The VCN has been reported to occur usually below −38 °C.[56,59] The temperature at which 50% cells with IIF during freezing the *Peromyscus* oocytes with ice-seeding is ~6.5 °C higher than that for freezing the cells without ice-seeding at 60 °C/min (−16.6 vs. −23.1 °C).

The above observations clearly indicate the significant role of extracellular ice in inducing IIF presumably through the surface (cell plasma membrane) catalyzed mechanism. An apparent difference between extracellular ice formed with controlled ice-seeding at a high subzero temperature and that formed stochastically as a result of deep subcooling is their morphology: The crystal of the latter is much finer than the former (see the images in Figs. 3 and 4). The fact that IIF was usually observed at a temperature less than 2–3 °C lower than that at which the stochastic formation of extracellular ice occurred (rather than up to ~40 °C lower than the seeding temperature) suggests that the fine ice crystal is much more effective to catalyze IIF than the big ice crystals growing out of ice embryos seeded at high subzero temperatures. This could be because the fine ice crystal is much more capable of penetrating through the plasma membrane (e.g., via aquapores[46]) into the cytoplasm to initiate IIF. If this is true, the effect of extracellular ice on IIF might not be as significant when VCN is the dominant mechanism of ice formation in the cells below −43 °C. Further studies to understand the impact of ice-seeding on volume catalyzed IIF are warranted. The better capability of the fine extracellular ice formed during freezing without ice-seeding may result in more nuclei and finer crystals of intracellular ice than the large extracellular ice formed during freezing with ice-seeding. During warming, the finer intracellular ice formed during freezing without ice-seeding may merge, which gave rise to the recrystallization phenomena presented in Fig. 4 (freezing without ice-seeding) while it was not observable for freezing with ice-seeding (Fig. 3).

Modeling of IIF

To enable us to obtain further understanding of the data on ice formation in *Peromyscus* oocytes shown in Fig. 5, the IIF model[56,59] given by Eqs. (3)–(6) were fit to the experimental data. In view of the wide temperature range from ~0 to −50 °C involved, the free volume theory-based model[26] given by Eqs. (7)–(8) were used to estimate the temperature-dependent viscosity of the cell cytoplasm. We first fit the data of P_{IIF} obtained under both freezing conditions (i.e., with and without ice-seeding) using the model assuming that SCN is the only ice nucleation mechanism. The fitting results are shown in Fig. 5 as dashed lines. Clearly, an excellent fit ($R^2 = 0.994$) was achieved for the data obtained by freezing without ice-seeding, suggesting that SCN should be the dominant mechanism of IIF when freezing the oocytes at 60 °C/min without ice-seeding.

For the condition with ice-seeding, however, the fitting was not as good ($R^2 = 0.975$) overall. Particularly, the single mechanism model cannot capture the sudden change of slope at the kink point (~−43 °C) at all, suggesting that more than one ice nucleation mechanism is involved over the wide temperature range under the condition with ice-seeding. Therefore, we further fitted the data obtained with ice-seeding using the model considering both SCN and VCN, and the results are shown in the figure as the solid line. Clearly, an excellent fit over the whole temperature range was achieved ($R^2 = 0.995$). Moreover, the fitting results clearly captured the sudden change of slope of the P_{IIF} data at the kink point. A further breakdown of the model prediction of P_{IIF} indicates that the sudden increase of slope below −43 °C was because of VCN of ice in the cells, while SCN dominated above −43 °C.

The two model parameters of SCN and VCN obtained for *Peromyscus* oocytes are further listed together with that reported in the literature for some other types of cells in Table 2. Clearly, the two parameters of SCN with ice-seeding for *Peromyscus*

TABLE 2. A comparison of the kinetic (Ω_0) and thermodynamic (κ_0) model parameters of both surface- and volume-catalyzed nucleations (SCN and VCN) of ice obtained in this study for *Peromyscus* oocytes either with or without ice-seeding and that reported in the literature for other cells during freezing with ice-seeding in the absence of cryoprotectant.

Cell type	Ref.	$\Omega_{0,\mathrm{SCN}}$, $\mathrm{m^{-2}\ s^{-1}}$	$\kappa_{0,\mathrm{SCN}}$, $\mathrm{K^5}$
SCN			
Peromyscus oocyte	This study		
Without ice-seeding		7.61×10^{10}	5.35×10^{10}
With ice-seeding		2.38×10^{7}	1.23×10^{9}
Mouse oocyte	Toner et al.[59]	3.56×10^{8}	4.6×10^{9}
Monkey oocyte	Younis et al. [66]	8×10^{8}	2.2×10^{9}
One-cell mouse embryo	Toner et al.[56]	8.2×10^{7}	7.8×10^{9}
D. melanogaster embryo	Myers et al.[49]	6×10^{5}	5.49×10^{9}
Islet β-cells	Toner[56]	7.5×10^{8}	1.0×10^{9}
Human μvascular–endothelial cells	Berrada and Bischof[3]	6.8×10^{8}	8.3×10^{9}
Hepatocyte (human)	Bischof et al.[5]	1.08×10^{9}	1.04×10^{9}
	Darr and Hubel[8]	7.6×10^{8}	7.5×10^{8}
Hepatocyte (pig)	Darr and Hubel[8]	1.3×10^{9}	4.8×10^{8}
Hepatocyte (rat)			
Suspended	Harris et al.[20]	1.1×10^{10}	1.4×10^{9}
Cultured (Day 7)	Yarmush et al.[65]	5.4×10^{9}	3×10^{8}
Digested (Day 7)	Yarmush et al.[65]	2.37×10^{10}	3.3×10^{8}
Smooth muscle cell (pig)	Balasubramanian et al.[1]		
Suspended		1.13×10^{8}	1.6×10^{9}
Monolayer		3.54×10^{10}	1.8×10^{9}
In fibrin matrix		3.78×10^{10}	2.1×10^{9}
Protoplast	Dowgert and Steponkus[12]		
Non-acclimated		1.5×10^{8}	3.4×10^{9}
Acclimated		1.1×10^{8}	1.6×10^{10}
		$\mathrm{m^{-3}\ s^{-1}}$	$\mathrm{K^5}$
VCN			
Peromyscus oocyte (with ice-seeding)	This study	2.87×10^{38}	1.32×10^{12}
Mouse oocyte	Toner et al.[59]	2.0×10^{50}	1.1×10^{12}
Erythrocyte	Mathias et al.[44]	1.0×10^{54}	1.7×10^{12}
Islet β-cell	Toner[56]	0.3×10^{32}	0.6×10^{12}
Acclimated protoplast	Fabbri[12]	1.6×10^{51}	1.5×10^{12}
D. melanogaster embryo	Myers et al.[49]	1×10^{49}	1.0×10^{12}

oocytes are within the usual range of the one reported in the literature for the various cells also with ice-seeding. However, the two parameters of SCN without ice-seeding are much higher than the literature data.

A high value of Ω_0 indicates that a high rate of IIF at high subzero temperatures, and a high value of κ_0 indicates a fast decrease of the rate of IIF with decreasing temperature according to Eq. (6). Therefore, the SCN-induced IIF during freezing without ice-seeding can be effectively depressed by cooling the cells using an extremely fast cooling/heating rate to allow minimum stay time in the high subzero temperature regimen, which is exactly the procedure of the emerging ultrafast cell vitrification technique using a much-reduced concentration (≤1.5–2.5 M) of cryoprotectant.[24,67] The two model parameters of VCN obtained for *Peromyscus* oocytes are within the usual range of the two parameters reported for the various cells in the literature.

For future study, the model parameters determined in this study will be important as the input to a model recently established for investigating the cell type-dependent, diffusion-limited intracellular ice nucleation and growth when freezing/cooling the *Peromyscus* oocytes in the presence of cryoprotectants,[64] for which experimental study using cryomicroscopy is difficult. The model together with the parameters determined in this study can be used to predict the percentage of IIF in *Peromyscus* oocytes under various CPA concentrations and cooling rates, which can be further correlated to the experimental data on cell survival under the various conditions. With such correlation being established, the model can be used to determine the desired CPA concentration to achieve a high survival of *Peromyscus* oocytes for a given cooling device (which determines the cooling rate during cryopreservation), and *vice versa*.

SUMMARY AND CONCLUSIONS

A systematic experimental and modeling study was performed to understand the water transport and IIF processes during freezing *Peromyscus* oocytes in culture medium without cryoprotectant as the first step toward cryopreservation of the *Peromyscus* oocytes, which has not been successful to date. It was found that the activation energy (E_{Lp}) for water transport across the plasma membrane of *Peromyscus* oocytes is high compared to that of other oocytes reported in the literature. Since a higher E_{Lp} indicates a stronger temperature dependence of the membrane water permeability, the water transport across the plasma membrane of *Peromyscus* oocytes is more strongly dependent on cooling rate than that of most other oocytes. It was further found that ice-seeding at a high subzero temperature has a profound impact on the kinetics of IIF in *Peromyscus* oocytes during freezing. With ice-seeding, IIF (surface-catalyzed) occurs at a much higher subzero temperature and over a much wider temperature range. Moreover, there is a change of the dominant mechanism (from surface- to volume-catalyzed nucleation i.e., SCN to VCN) of IIF at ~−43 °C with ice-seeding. The kinetic (Ω_0) and thermodynamic (κ_0) model parameters of surface-catalyzed ice nucleation during freezing without ice-seeding are much higher than that during freezing with ice-seeding. Since a higher κ_0 indicates a stronger temperature dependence of the nucleation rate of IIF, IIF should be able to be effectively depressed by using an ultrafast cooling/heating rate to minimize the stay time at high subzero temperatures when cryopreserving the cells by vitrification (without ice-seeding). The microscopic observations and the model parameters indicate the importance of quantifying the IIF kinetics in the absence of ice-seeding during cooling for developing optimal vitrification protocols of cell cryopreservation.

ACKNOWLEDGMENTS

This study was partially supported by the South Carolina Research Foundation (NSF RII # EPS-0447660), the Chinese Ministry of Education for a joint doctoral training program, and NIH/NCRR (#P40 RR014279). The authors would like to thank Kyle Gilstrap for proofreading the manuscript.

REFERENCES

[1]Balasubramanian, S. K., R. T. Venkatasubramanian, A. Menon, and J. C. Bischof. Thermal injury prediction during cryoplasty through in vitro characterization of smooth muscle cell biophysics and viability. *Ann. Biomed. Eng*. 36:86–101, 2008.

[2]Benson, C. T., and J. K. Critser. Variation of water permeability (Lp) and its activation energy (Ea) among unfertilized golden hamster and ICR murine oocytes. *Cryobiology* 31:215–223, 1994.

[3]Berrada, M. S., and J. C. Bischof. Evaluation of freezing effects on human microvascular-endothelial cells (HMEC). *Cryo Letters* 22:353–366, 2001.

[4]Bischof, J. C. Quantitative measurement and prediction of biophysical response during freezing in tissues. *Annu. Rev. Biomed. Eng*. 2:257–288, 2000.

[5]Bischof, J. C., C. M. Ryan, R. G. Tompkins, M. L. Yarmush, and M. Toner. Ice formation in isolated human hepatocytes and human liver tissue. *ASAIO J*. 43:271–278, 1997.

[6]Chen, S. U., Y. R. Lien, H. F. Chen, K. H. Chao, H. N. Ho, and Y. S. Yang. Open pulled straws for vitrification of mature mouse oocytes preserve patterns of meiotic spindles

and chromosomes better than conventional straws. *Hum. Reprod.* 15:2598–2603, 2000.
[7]Chen, S. U., Y. R. Lien, Y. Y. Cheng, H. F. Chen, H. N. Ho, and Y. S. Yang. Vitrification of mouse oocytes using closed pulled straws (CPS) achieves a high survival and preserves good patterns of meiotic spindles, compared with conventional straws, open pulled straws (OPS) and grids. *Hum. Reprod.* 16:2350–2356, 2001.
[8]Darr, T. B., and A. Hubel. Freezing characteristics of isolated pig and human hepatocytes. *Cell Transplant.* 6:173–183, 1997.
[9]Dessolle, L., V. de Larouziere, C. Ravel, I. Berthaut, J. M. Antoine, and J. Mandelbaum. Slow freezing and vitrification of human mature and immature oocytes. *Gynecol. Obstet. Fertil.* 37:712–719, 2009.
[10]Devireddy, R. V., J. E. Coad, and J. C. Bischof. Microscopic and calorimetric assessment of freezing processes in uterine fibroid tumor tissue. *Cryobiology* 42:225–243, 2001.
[11]Devireddy, R. V., D. Raha, and J. C. Bischof. Measurement of water transport during freezing in cell suspensions using a differential scanning calorimeter. *Cryobiology* 36:124–155, 1998.
[12]Dowgert, M. F., and P. L. Steponkus. Effect of cold acclimation on intracellular ice formation in isolated protoplasts. *Plant Physiol.* 72:978–988, 1983.
[13]Fabbri, R. Cryopreservation of human oocytes and ovarian tissue. *Cell Tissue Bank* 7:113–122, 2006.
[14]Fahy, G. M., D. R. MacFarlane, C. A. Angell, and H. T. Meryman. Vitrification as an approach to cryopreservation. *Cryobiology* 21:407–426, 1984.
[15]Fahy, G. M., B. Wowk, J. Wu, and S. Paynter. Improved vitrification solutions based on the predictability of vitrification solution toxicity. *Cryobiology* 48:22–35, 2004.
[16]Fowler, A., and M. Toner. Cryo-injury and biopreservation. *Ann. N. Y. Acad. Sci.* 1066:119–135, 2005.
[17]Fray, M. D. Biological methods for archiving and maintaining mutant laboratory mice. Part I: conserving mutant strains. *Methods Mol. Biol.* 561:301–319, 2009.
[18]Gardner, D. K., C. B. Sheehan, L. Rienzi, M. Katz-Jaffe, and M. G. Larman. Analysis of oocyte physiology to improve cryopreservation procedures. *Theriogenology* 67:64–72, 2007.
[19]Han, B., and J. C. Bischof. Engineering challenges in tissue preservation. *Cell Preserv. Technol.* 2:91–112, 2004.
[20]Harris, C. L., M. Toner, A. Hubel, E. G. Cravalho, M. L. Yarmush, and R. G. Tompkins. Cryopreservation of isolated hepatocytes: intracellular ice formation under various chemical and physical conditions. *Cryobiology* 28:436–444, 1991.
[21]He, X., and J. C. Bischof. Quantification of temperature and injury response in thermal therapy and cryosurgery. *Crit. Rev. Biomed. Eng.* 31:355–422, 2003.
[22]He, X., and J. C. Bischof. The kinetics of thermal injury in human renal carcinoma cells. *Ann. Biomed. Eng.* 33:502–510, 2005.
[23]He, X., S. McGee, J. E. Coad, F. Schmidlin, P. A. Iaizzo, D. J. Swanlund, S. Kluge, E. Rudie, and J. C. Bischof. Investigation of the thermal and tissue injury behaviour in microwave thermal therapy using a porcine kidney model. *Int. J. Hyperthermia* 20:567–593, 2004.
[24]He, X., E. Y. Park, A. Fowler, M. L. Yarmush, and M. Toner. Vitrification by ultra-fast cooling at a low concentration of cryoprotectants in a quartz micro-capillary: a study using murine embryonic stem cells. *Cryobiology* 56:223–232, 2008.
[25]He, X., W. F. Wolkers, J. H. Crowe, D. J. Swanlund, and J. C. Bischof. In situ thermal denaturation of proteins in dunning AT-1 prostate cancer cells: implication for hyperthermic cell injury. *Ann. Biomed. Eng.* 32:1384–1398, 2004.
[26]He, X. M., A. Fowler, and M. Toner. Water activity and mobility in solutions of glycerol and small molecular weight sugars: Implication for cryo- and lyopreservation. *J. Appl. Phys.* 100:074702, 2006 (074711 pp).
[27]Heng, B. C., L. L. Kuleshova, S. M. Bested, H. Liu, and T. Cao. The cryopreservation of human embryonic stem cells. *Biotechnol. Appl. Biochem.* 41:97–104, 2005.
[28]Himmelblau, D. M. Applied Nonlinear Programming. New York: McGraw-Hill Inc., 1972.
[29]Hunt, C. J., D. E. Pegg, and S. E. Armitage. Optimising cryopreservation protocols for haematopoietic progenitor cells: a methodological approach for umbilical cord blood. *Cryoletters* 27:73–83, 2006.
[30]Hunter, J., A. Bernard, B. Fuller, J. McGrath, and R. W. Shaw. Plasma membrane water permeabilities of human oocytes: the temperature dependence of water movement in individual cells. *J. Cell. Physiol.* 150:175–179, 1992.
[31]Hunter, J. E., A. Bernard, B. J. Fuller, J. J. McGrath, and R. W. Shaw. Measurements of the membrane water permeability (Lp) and its temperature dependence (activation energy) in human fresh and failed-to-fertilize oocytes and mouse oocyte. *Cryobiology* 29:240–249, 1992.
[32]Jain, J. K., and R. J. Paulson. Oocyte cryopreservation. *Fertil. Steril.* 86(Suppl 4):1037–1046, 2006.
[33]Jeruss, J. S., and T. K. Woodruff. Preservation of fertility in patients with cancer. *N. Engl. J. Med.* 360:902–911, 2009.
[34]Karlsson, J. O. M., E. G. Cravalho, and M. Toner. A model of diffusion-limited ice growth inside biological cells during freezing. *J. Appl. Phys.* 75:4442–4445, 1994.
[35]Karlsson, J. O., A. I. Younis, A. W. Chan, K. G. Gould, and A. Eroglu. Permeability of the rhesus monkey oocyte membrane to water and common cryoprotectants. *Mol. Reprod. Dev.* 76:321–333, 2009.
[36]Kleinhans, F. W., and P. Mazur. Determination of the water permeability (Lp) of mouse oocytes at −25 degrees C and its activation energy at subzero temperatures. *Cryobiology* 58:215–224, 2009.
[37]Kouba, A. J., and C. K. Vance. Applied reproductive technologies and genetic resource banking for amphibian conservation. *Reprod. Fertil. Dev.* 21:719–737, 2009.
[38]Leibo, S. P. Water permeability and its activation energy of fertilized and unfertilized mouse ova. *J. Membr. Biol.* 53:179–188, 1980.
[39]Leibo, S. P., and N. Songsasen. Cryopreservation of gametes and embryos of non-domestic species. *Theriogenology* 57:303–326, 2002.
[40]Levin, R. L., E. G. Cravalho, and C. E. Huggins. A membrane model describing the effect of temperature on the water conductivity of erythrocyte membranes at subzero temperatures. *Cryobiology* 13:415–429, 1976.
[41]Litkouhi, B., D. Marlow, J. J. McGrath, and B. Fuller. The influence of cryopreservation on murine oocyte water permeability and osmotically inactive volume. *Cryobiology* 34:23–35, 1997.
[42]Mandelbaum, J., J. Belaisch-Allart, A. M. Junca, J. M. Antoine, M. Plachot, S. Alvarez, M. O. Alnot, and J. Salat-Baroux. Cryopreservation in human assisted reproduction is now routine for embryos but remains a research procedure for oocytes. *Hum. Reprod.* 13(Suppl 3): 161–174, 1998.

[43]Manipalviratn, S., and A. Decherney. Clinical application of human oocyte cryopreservation. *Rev. Recent Clin. Trials* 3:104–110, 2008.
[44]Mathias, S. F., F. Franks, and K. Trafford. Nucleation and growth of ice in deeply undercooled erythrocytes. *Cryobiology* 21:123–132, 1984.
[45]Mazur, P. Kinetics of water loss from cells at subzero temperatures and the likelihood of intracellular freezing. *J. Gen. Physiol.* 47:347–369, 1963.
[46]Mazur, P. The role of cell membranes in the freezing of yeast and other single cells. *Ann. N. Y. Acad. Sci.* 125:658–676, 1965.
[47]Mazur, P. Freezing of living cells: mechanisms and implications. *Am. J. Physiol.* 247:C125–142, 1984.
[48]Mazur, P., S. P. Leibo, and G. E. Seidel, Jr. Cryopreservation of the germplasm of animals used in biological and medical research: importance, impact, status, and future directions. *Biol. Reprod.* 78:2–12, 2008.
[49]Myers, S. P., R. E. Pitt, D. V. Lynch, and P. L. Steponkus. Characterization of intracellular ice formation in Drosophila melanogaster embryos. *Cryobiology* 26:472–484, 1989.
[50]Nagy, Z. P., C. C. Chang, D. B. Shapiro, D. P. Bernal, H. I. Kort, and G. Vajta. The efficacy and safety of human oocyte vitrification. *Semin. Reprod. Med.* 27: 450–455, 2009.
[51]Pedro, P. B., E. Yokoyama, S. E. Zhu, N. Yoshida, D. M. Valdez, Jr., M. Tanaka, K. Edashige, and M. Kasai. Permeability of mouse oocytes and embryos at various developmental stages to five cryoprotectants. *J. Reprod. Dev.* 51:235–246, 2005.
[52]Porcu, E., and S. Venturoli. Progress with oocyte cryopreservation. *Curr. Opin. Obstet. Gynecol.* 18:273–279, 2006.
[53]Rall, W. F., and G. M. Fahy. Ice-free cryopreservation of mouse embryos at −196-degrees-C by vitrification. *Nature* 313:573–575, 1985.
[54]Ruffing, N. A., P. L. Steponkus, R. E. Pitt, and J. E. Parks. Osmometric behavior, hydraulic conductivity, and incidence of intracellular ice formation in bovine oocytes at different developmental stages. *Cryobiology* 30:562–580, 1993.
[55]Schwartz, G. J., and K. R. Diller. Analysis of the water permeability of human granulocytes at subzero temperatures in the presence of extracellular ice. *J. Biomech. Eng.* 105:360–366, 1983.
[56]Toner, M. Nucleation of ice crystals inside biological cells. *Adv. Low-Temp. Biol.* 2:1–51, 1993.
[57]Toner, M., and E. G. Cravalho. Thermodynamics and kinetics of intracellular ice formation during freezing of biological cells. *J. Appl. Phys.* 67:1582–1593, 1990.
[58]Toner, M., E. G. Cravalho, and D. R. Armant. Water transport and estimated transmembrane potential during freezing of mouse oocytes. *J. Membr. Biol.* 115:261–272, 1990.
[59]Toner, M., E. G. Cravalho, and M. Karel. Thermodynamics and kinetics of intracellular ice formation during freezing of biological cells. *J. Appl. Phys.* 67:1582–1593, 1990.
[60]Toner, M., E. G. Cravalho, M. Karel, and D. R. Armant. Cryomicroscopic analysis of intracellular ice formation during freezing of mouse oocytes without cryoadditives. *Cryobiology* 28:55–71, 1991.
[61]Trounson, A., and L. Mohr. Human pregnancy following cryopreservation, thawing and transfer of an eight-cell embryo. *Nature* 305:707–709, 1983.
[62]Vajta, G., and Z. P. Nagy. Are programmable freezers still needed in the embryo laboratory? Review on vitrification. *Reprod. Biomed. Online* 12:779–796, 2006.
[63]Veres, M., A. R. Duselis, A. Graft, M. J. Dewey, J. Crossland, P. B. Vrana, and G. Szalai. The biology and methodology of assisted reproduction in deer mice (Peromyscus maniculatus). *Theriogenology* 2010 (under review).
[64]Yang, G., A. Zhang, L. X. Xu, and X. He. Modeling the cell-type dependence of diffusion-limited intracellular ice nucleation and growth during both vitrification and slow freezing. *J. Appl. Phys.* 105:114701–114711, 2009.
[65]Yarmush, M. L., M. Toner, J. C. Dunn, A. Rotem, A. Hubel, and R. G. Tompkins. Hepatic tissue engineering. Development of critical technologies. *Ann. N. Y. Acad. Sci.* 665:238–252, 1992.
[66]Younis, A. I., M. Toner, D. F. Albertini, and J. D. Biggers. Cryobiology of non-human primate oocytes. *Hum. Reprod.* 11:156–165, 1996.
[67]Zhang, W., G. Yang, A. Zhang, L. X. Xu, and X. He. Preferential vitrification of water in small alginate microcapsules significantly augments cell cryopreservation by vitrification. *Biomed. Microdevices* 12:89–96, 2010.